Endothelin-2 signaling in the neural retina promotes the endothelial tip cell state and inhibits angiogenesis

Amir Rattner[a,1], Huimin Yu[a], John Williams[a,b], Philip M. Smallwood[a,b], and Jeremy Nathans[a,b,c,d,1]

Departments of [a]Molecular Biology and Genetics, [c]Neuroscience, and [d]Ophthalmology and [b]Howard Hughes Medical Institute, Johns Hopkins University School of Medicine, Baltimore, MD 21205

Contributed by Jeremy Nathans, August 20, 2013 (sent for review February 19, 2013)

Endothelin signaling is required for neural crest migration and homeostatic regulation of blood pressure. Here, we report that constitutive overexpression of Endothelin-2 (Edn2) in the mouse retina perturbs vascular development by inhibiting endothelial cell migration across the retinal surface and subsequent endothelial cell invasion into the retina. Developing endothelial cells exist in one of two states: tip cells at the growing front and stalk cells in the vascular plexus behind the front. This division of endothelial cell states is one of the central organizing principles of angiogenesis. In the developing retina, Edn2 overexpression leads to overproduction of endothelial tip cells by both morphologic and molecular criteria. Spatially localized overexpression of Edn2 produces a correspondingly localized endothelial response. Edn2 overexpression in the early embryo inhibits vascular development at midgestation, but Edn2 overexpression in developing skin and brain has no discernible effect on vascular structure. Inhibition of retinal angiogenesis by Edn2 requires expression of Endothelin receptor A but not Endothelin receptor B in the neural retina. Taken together, these observations imply that the neural retina responds to Edn2 by synthesizing one or more factors that promote the endothelial tip cell state and inhibit angiogenesis. The response to Edn2 is sufficiently potent that it overrides the activities of other homeostatic regulators of angiogenesis, such as Vegf.

The architecture of the vertebrate vasculature has long been an object of fascination for biologists. At a macroscopic scale, the trajectories and branch points of major arteries and veins are highly stereotyped, and at a microscopic scale, capillary density within each tissue is governed by characteristic statistical parameters. These attributes are particularly accessible to observation and manipulation in the mammalian retina (1, 2). In many mammals, including mice and humans, the retinal vasculature develops by radial migration of endothelial cells (ECs) along the inner (vitreal) face of the retina starting from their point of entry at the optic disk. In a second phase of development, branches from the primary vascular plexus penetrate into the retina to form two parallel tiers of capillaries that flank a central layer of retinal neurons, the inner nuclear layer (INL). During both phases, EC proliferation and migration are driven, at least in part, by tissue-derived Vegf (3, 4).

During radial growth, there is a clear morphologic distinction between ECs at the growing front of the vascular plexus, referred to as tip cells, and the bulk of the ECs that follow behind the front, referred to as stalk cells (5). In particular, tip cells possess numerous filopodia and are highly motile, acting like the vascular equivalent of axonal growth cones. Stalk cells proliferate, but they lack filopodia. The balance between tip and stalk cell states is orchestrated by asymmetric signaling through the Notch pathway: tip cells express the Notch ligand Δ-like4 (Dll4), which acts on stalk cell Notch receptors to decrease stalk-to-tip conversion, whereas stalk cells express the Notch ligand Jagged1, which antagonizes Dll4 activity (6, 7). This pathway is intimately linked to Vegf signaling; Vegfa promotes Dll4 expression in tip cells, and Notch signaling in stalk cells suppresses the response to Vegfa. Additionally, Vegfa, acting through Vegfr2, directly promotes the tip cell fate, including filopodia formation. Recent time lapse imaging studies of vascular development in zebrafish and mammalian EC dynamics in explant culture show that the tip cell and stalk cell states are highly plastic, with frequent exchanges between the two cell states (8, 9).

Several other signaling pathways are also essential for retinal vascular development. Norrin, a Muller-glia–derived ligand, and its EC receptor Frizzled4 (Fz4), coreceptor Lrp5, and receptor chaperone Tspan12 activate canonical Wnt signaling in developing ECs (10). In humans and mice, defects in any of these components lead to retinal hypovascularization. Similar phenotypes are observed in mice lacking Angiopoietin2 (Ang2), an antagonist of the Tie2 receptor tyrosine kinase, or overexpressing leukemia inhibitory factor (11–13).

Interest in retinal vascular development is motivated, in part, by the central role that neovascularization plays in age-related macular degeneration and diabetic retinopathy, two of the most prevalent adult-onset eye diseases (14). The success of anti-Vegf therapies in treating these disorders has motivated the search for additional regulators of retinal vascular growth (15).

The experiments reported here focus on the effects of endothelin signaling on retinal vascular development. Endothelins were initially discovered as endogenous vasoconstricting peptides (16). In mammals, there are three closely related peptides [Endothelin-1 (Edn1), Edn2, and Edn3], each of which is encoded by a distinct gene and released by proteolysis from a large polypeptide precursor. Two G protein-coupled receptors, Ednra and Ednrb, mediate the effects of the endothelins. In addition to their roles in homeostatic regulation of blood pressure—including regulation of arterial smooth muscle tone, renal fluid and salt retention, and cardiac contractility—endothelins and endothelin receptors play critical roles in neural crest migration (17). In mice and humans, defects in *Edn3* or *Ednrb* lead to

Significance

Two distinct and interconvertible types of endothelial cells are present during blood vessel growth: tip cells at the growing front of the vascular network and stalk cells behind the front. In the present study, overexpression of Endothelin-2, a peptide previously implicated in the control of blood pressure, is shown to promote the tip cell fate and arrest vascular growth within the mouse retina. Genetic experiments show that this effect requires Endothelin receptor A expression in the neural retina, implying the existence of a retina-derived regulator of vascular growth and development that is under Endothelin control.

Author contributions: A.R. and J.N. designed research; A.R., H.Y., J.W., P.M.S., and J.N. performed research; A.R. and J.N. analyzed data; and J.N. wrote the paper.

The authors declare no conflict of interest.

Data deposition: The sequence reported in this paper has been deposited in the Gene Expression Omnibus (GEO) database, www.ncbi.nlm.nih.gov/geo (accession no. GSE50059) and the NCBI sequence read archive, www.ncbi.nlm.nih.gov/sra (accession no. SRP029473).

[1]To whom correspondence may be addressed. E-mail: jnathans@jhmi.edu or arattner@jhmi.edu.

This article contains supporting information online at www.pnas.org/lookup/suppl/doi:10.1073/pnas.1315509110/-/DCSupplemental.

deficiencies in skin melanocytes and enteric neurons in the colon, both of which are neural crest derivatives. In mice, defects in *Edn1* or *Ednra* lead to deficiencies in cranial and cardiac neural crest derivatives, with resulting deficiencies in craniofacial and cardiac outflow tract development, respectively. Mutations in *Edn2* have not been reported.

In earlier work, we and others identified *Edn2* transcripts among a small set of transcripts that increase in abundance in injured or diseased photoreceptors (18–20). This induction is observed in a wide variety of experimental paradigms, including retinal detachment, light damage, and inherited photoreceptor degeneration. Here we report the surprising discovery that Edn2 overexpression in the developing mouse retina potently and specifically inhibits retinal angiogenesis and promotes the tip cell state.

Results

Edn2 Overexpression in the Retina Inhibits Vascular Development. Our point of departure for the experiments described below was the generation of a knockin mouse line at the Ubiquitin-b locus that directs the expression of Edn2 from a CMV/β-actin (CAG) promoter after Cre-mediated excision of a *loxP-stop-loxP* cassette (Fig. S1*A*). With this allele, referred to as *Z/Edn2*, expression is possible in virtually any cell type and at any time during development, and is determined by the expression pattern of the Cre driver.

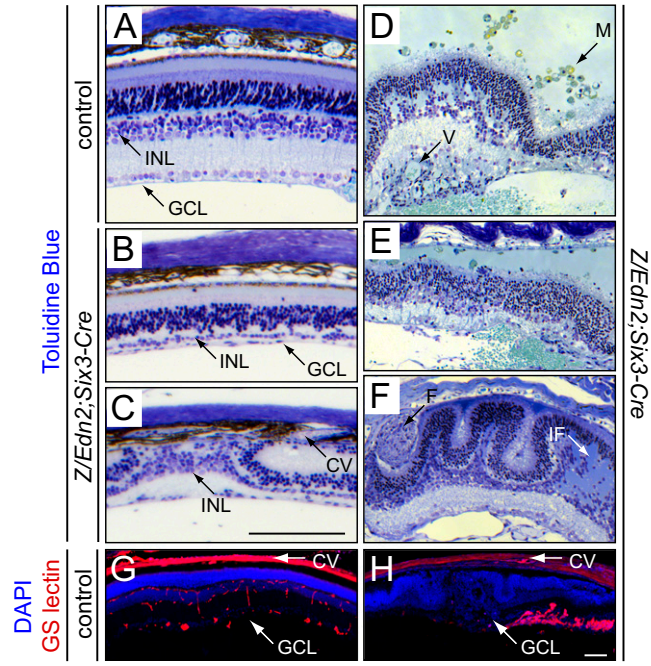

Fig. 1. Retinal vascular defects in *Z/Edn2;Six3-Cre* mice. (*A–F*) Sections of (*A*) adult control and (*B–F*) *Z/Edn2;Six3-Cre* retinas stained with Toluidine Blue reveal a range of defects that presumably result from hypovascularization, including (*B*) retinal thinning, (*C*) disorganization of retinal layers and choroidal neovascularization, (*D* and *E*) retinal detachments with accumulation of macrophages in the subretinal space, and (*F*) retinal folds with subretinal fibrosis and enlarged superficial blood vessels. In these sections and all other retinal sections, the retinal pigment epithelium is at the top, and the ganglion cell layer (GCL) is at the bottom. CV, choroidal vasculature; F, fibrosis; IF, interstitial fluid; M, macrophage; V, vessel. [Scale bar: *C* (refers to *A–F*), 100 μm.] (*G* and *H*) Fresh frozen sections of (*G*) adult control and (*H*) *Z/Edn2;Six3-Cre* retinas stained with GS-lectin (Isolectin B4) to visualize the vasculature. The *Z/Edn2;Six3-Cre* retina lacks intraretinal capillaries, and the superficial vasculature extends from the right only to the midpoint of the image. (Scale bar: 100 μm.)

In *Z/Edn2;Six3-Cre* mice, Edn2 is produced throughout the developing and mature retina beginning at approximately embryonic day 11 (E11). An examination of adult *Z/Edn2;Six3-Cre* retinas revealed diverse morphologic defects (Fig. 1). Some retinal regions are very thin, especially the ganglion cell layer and INL (compare Fig. 1*A* with Fig. 1*B*) or less commonly, the outer nuclear layer (ONL) (Fig. 1*C*). [Throughout this paper, control retinas are derived from age-matched and phenotypically WT mice—typically littermates—that carry a subset of the genetic markers of the experimental mice.] Other retinal regions exhibit extensive detachment, with numerous macrophages occupying the subretinal space, severe folding of the retina, accumulation of interstitial fluid, and/or development of interstitial fibrosis (Fig. 1 *D–F*). In some regions, few or no blood vessels were observed on the vitreal face of the retina (Fig. 1 *B* and *C*), whereas in other regions, clusters of blood vessels occupy the vitreal face (Fig. 1*D*). It is unclear whether these retina-associated vessels were initially derived from bona fide retinal vasculature or recruited from the hyaloid vasculature, a transient vascular plexus within the developing vitreous. Visualizing the vasculature with *Griffonia simplicifolia* (GS)-lectin binding confirmed these observations and also showed an absence of the normal intraretinal capillary beds in the IPL and OPL (compare Fig. 1*G* with Fig. 1*H*).

To characterize vascular development in the *Z/Edn2;Six3-Cre* retina, we visualized ECs and astrocytes at different postnatal ages in flat-mount retinas (Fig. 2). At postnatal day 3 (P3) and P6, the expanding front of the astrocyte network was modestly retarded in *Z/Edn2;Six3-Cre* retinas relative to littermate controls, but this differential disappeared by P8 (Fig. 2 *A–E*). However, EC growth was significantly retarded in *Z/Edn2;Six3-Cre* retinas at all postnatal ages examined, with the radial position of the growing ECs largely arrested by ∼P6 (Fig. 2 *A–E*). Despite their severely retarded radial migration, *Z/Edn2;Six3-Cre* ECs associate with astrocytes in a manner closely resembling control retinas (Fig. 2 *F* and *G*). In adult *Z/Edn2;Six3-Cre* retinas, the density of mural cell coverage of the EC network is similar to controls, which was determined by immunostaining for NG2. The overall density of astrocytes and ECs in the vascularized territory of *Z/Edn2;Six3-Cre* retinas is several fold higher than in controls (Fig. 2 *A–D*).

As noted in the Introduction, in the radially expanding early postnatal retinal vasculature, there are two morphologically and molecularly distinct classes of endothelial cells (5, 21). Tip cells are located at the growing front, produce numerous filopodia, and lack a lumen. They also produce the paracrine ligand Apelin (Apln) and the Notch ligand Dll4, and they repress the Angiopoetin receptor Tie2. Stalk cells are located behind the growing front, lack filopodia, develop a luminal cavity, and form junctional complexes with neighboring stalk cells to create a capillary network; they express Tie2 but do not express Apln or Dll4. High-resolution imaging of P6 retinal flat mounts immunostained for the endothelial plasma membrane protein PECAM1 revealed the presence of filopodia-bearing ECs throughout much of the growing vascular plexus in *Z/Edn2;Six3-Cre* retinas, whereas control retinas show filopodia predominantly at the growing front (Fig. 2 *H* and *I*). A quantitative comparison of filopodial density in the interior of developing WT with *Z/Edn2;Six3-Cre* vascular networks is hampered by the higher mean density of ECs in the *Z/Edn2;Six3-Cre* plexus, which leaves far smaller cell-free spaces in which to observe the filopodia. With filopodia differentially scored based on their location at the vascular front or the interior, we observed a several fold higher density of filopodia in the interior of the *Z/Edn2;Six3-Cre* vascular plexus at P7 compared with the controls (Fig. S2).

To measure the patency of the developing EC network, we used two methods. In the first method, we injected a small volume of highly concentrated Alexa595-GS-lectin into the beating

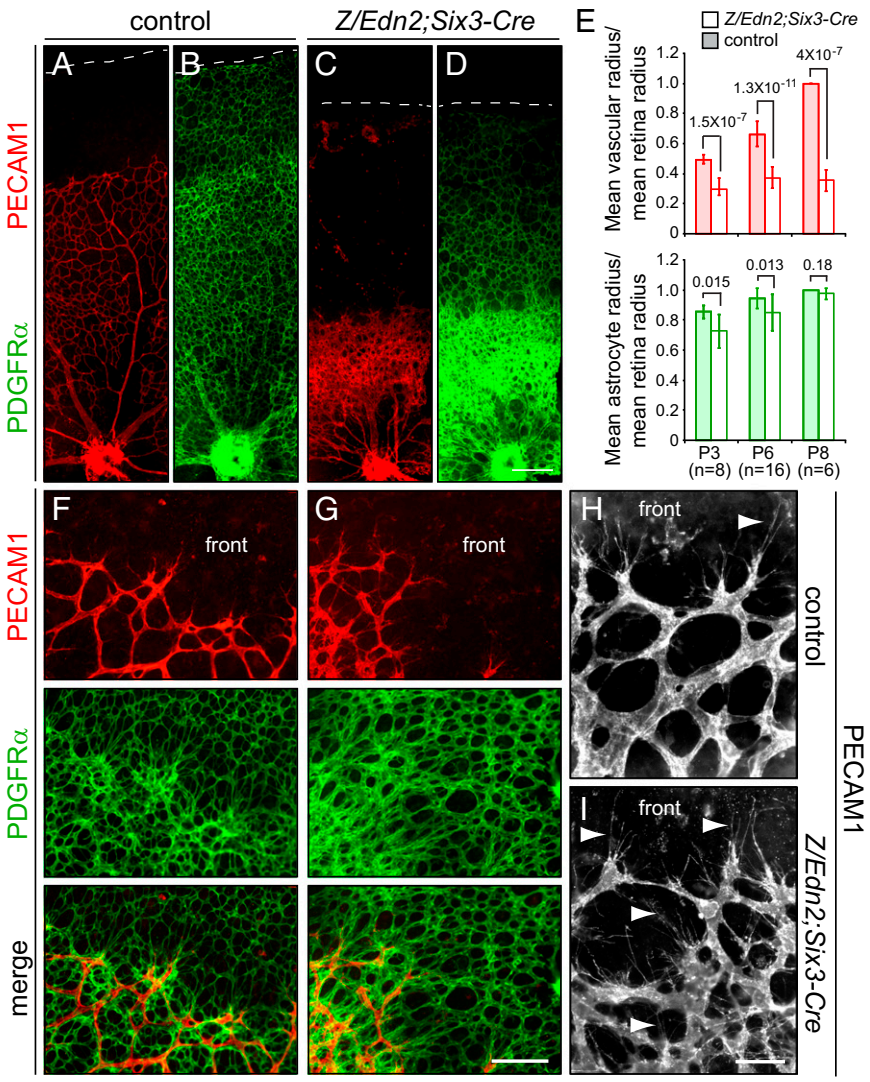

Fig. 2. Inhibition of vascular growth and production of excess tip cells in *Z/Edn2;Six3-Cre* retinas. (*A–D*) Flat-mount retinas from P6 control and *Z/Edn2;Six3-Cre* mice immunostained for PECAM1 (ECs) and PDGFRα (astrocytes). The optic disk is at the bottom of each image. Dashed lines mark the edge of the developing retina. (Scale bar: 200 μm.) (*E*) Quantification of the fraction of retinal surface area covered by blood vessels and astrocytes in control and *Z/Edn2;Six3-Cre* retinas at P3, P6, and P8. For each retina, distances were measured from the optic disk to the edge of the developing vasculature, the astrocyte network, and the retina along three directions, and the ratios were averaged. The histograms show the mean and SD of measurements from the indicated number of retinas (*n*) with corresponding *P* values. (*F* and *G*) High-magnification images of the leading edge of the developing vasculature in flat-mount control and *Z/Edn2;Six3-Cre* retinas at P6 stained as in *A–D*. In both cases, ECs grow along the astrocyte network. (Scale bar: 100 μm.) (*H* and *I*) High-magnification images of ECs at the leading edge of the developing vasculature in flat-mount control and *Z/Edn2;Six3-Cre* retinas at P6 immunostained for PECAM1. (*H*) In control retinas, filopodia (arrowheads) are confined to tip cells at the front. (*I*) In *Z/Edn2;Six3-Cre* retinas, filopodia are on ECs at the vascular front and within the vascular plexus. (Scale bar: 50 μm.)

hearts of deeply anesthetized mice (four *Z/Edn2;Six3-Cre* and five control mice at P5–P7). After waiting 5 min for the GS-lectin to fill and bind to the patent vasculature, the eyes were excised and fixed, and the isolated retinas were detergent-permeabilized. Then, the entire retinal vasculature was labeled with Alexa488-GS-lectin. In the second method, the circulatory system was perfused with DiI, a hydrophobic carbocyanine dye, through cardiac puncture and under external pressure (22), after which the retinal vasculature was visualized by GS-lectin binding without detergent and promptly imaged (two *Z/Edn2;Six3-Cre* and three control mice at P7 and one *Z/Edn2;Six3-Cre* and one control at P11). Fig. 3 shows that, in control retinas, the perfused fluorescent reporters label the vascular plexus uniformly and within one to three cell diameters of the growing front. In contrast, in *Z/Edn2;Six3-Cre* retinas, perfusion is limited to a territory that is 5–15 cell diameters behind the growing vascular front and is spatially heterogeneous. In keeping with this perfusion deficit, tissue hypoxia—as measured by the accumulation of pimonidazole (Hypoxyprobe) (23)—was substantial in the *Z/Edn2;Six3-Cre* retina, both in front of and beneath the developing vascular plexus (Fig. 3 *F* and *G*).

Molecular and Cellular Responses to Edn2: A Bias to the Tip Cell State. To extend the morphologic and functional analyses described in the preceding section to the molecular level, we compared transcript abundances and localizations in control versus *Z/Edn2;Six3-Cre* retinas. These analyses were performed on P5–P8 retinas during the period of rapid endothelial growth. At P6 there are large numbers of patent vessels at the vitreal surface of the control retina, with larger vessels overlying the central retina and smaller vessels overlying the peripheral retina (Fig. 4*A*, *Left*). In keeping with the data shown in Figs. 2 and 3, near the center of the *Z/Edn2;Six3-Cre* retina, there are both patent vessels and masses of ECs without luminal spaces (Fig. 4*A*, *Upper Right*), whereas in the peripheral retina, ECs are entirely absent from the vitreal surface (Fig. 4*A*, *Lower Right*). The peripheral *Z/Edn2;Six3-Cre* retina is also thinner than the control at P6.

Whole-retina transcriptome analyses were performed using both microarray hybridization at P8 and RNAseq at P5; the two methods gave largely congruent results (Fig. 4 *B* and *C* and Tables S1–S4). Based on the histologic analyses described above, we expect transcriptome differences to reflect a combination of the following perturbations in the *Z/Edn2;Six3-Cre* retina: (*i*) Edn2-mediated regulation of gene expression in the retina and/or vasculature, (*ii*) retinal hypoxia, and (*iii*) excess of tip cells. As expected, *Edn2* coding sequences were present at far higher abundances (~100-fold) in *Z/Edn2;Six3-Cre* compared with control retina, which was determined by RNAseq. (No differences in *Edn2* transcript abundance were registered in the microarray analysis, because all of the *Edn2* oligonucleotide probe sets in

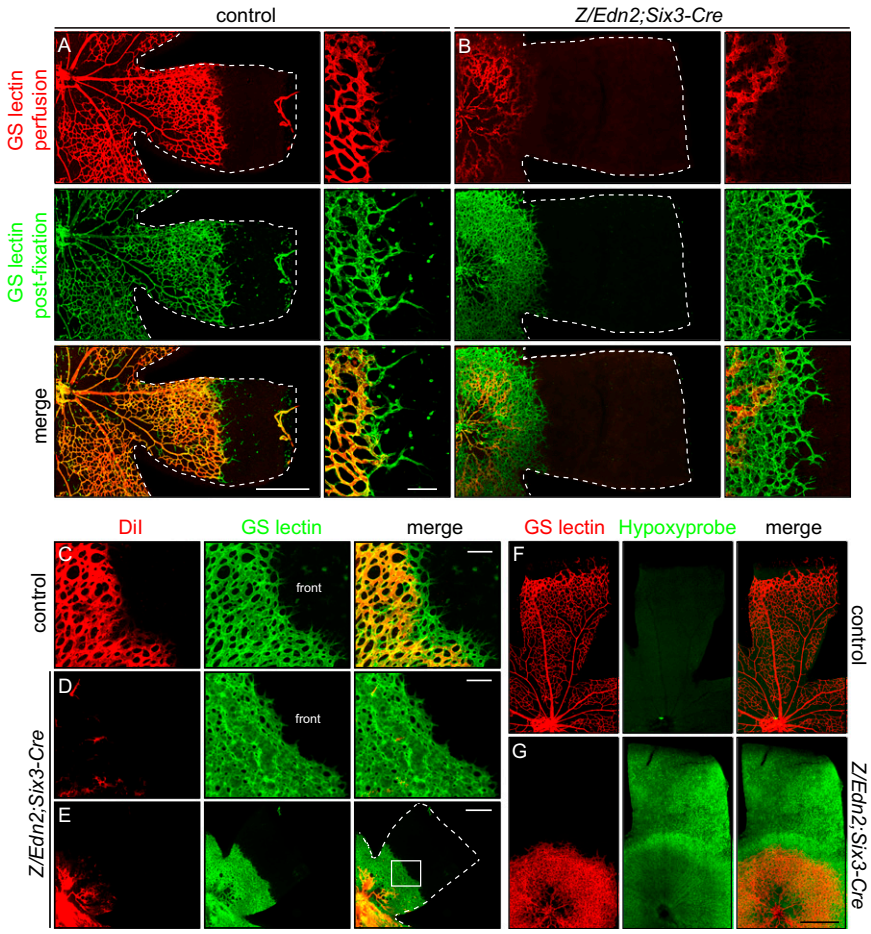

Fig. 3. In developing *Z/Edn2;Six3-Cre* retinas, large regions of the EC network are not perfused. (*A* and *B*) Retina flat mounts from (*A*) control and (*B*) *Z/Edn2;Six3-Cre* retinas at P6 after intracardiac injection of Alexa595 GS-lectin and postfixation permeabilization and labeling with Alexa488 GS-lectin. *Right* shows an enlargement of the region at the vascular front (*Left*). The dashed line delineates the edge of the developing retina in *A*, *B*, and *E*. (Scale bars: *Left*, 500 μm; *Right*, 100 μm.) (*C*–*E*) Flat mounts showing the front of the developing vasculature in (*C*) control and (*D* and *E*) *Z/Edn2;Six3-Cre* retinas at P7 after intracardiac perfusion of DiI. The white square in *E* corresponds to the region shown in *D*. (Scale bars: *C* and *D*, 100 μm; *E*, 500 μm.) (*F* and *G*) Hypoxyprobe labeling of (*F*) control and (*G*) *Z/Edn2;Six3-Cre* retinas at P7. (Scale bar: 500 μm.)

the Affimetrix version 430 2.0 gene chip are derived from the *Edn2* 3′ UTR, which was not included in the *Z/Edn2* knockin.) More interestingly, the stalk cell markers Tie2 and Apj (the G protein-coupled receptor for Apln) were underrepresented in the *Z/Edn2;Six3-Cre* retina transcriptome as were the transporters Slco1c1 and Slc38a5 (mediators of thyroid hormone and neutral amino acid uptake, respectively) and transcription factor Sox17, which was suggested by earlier work to be a regulator of retinal vascular development in response to Norrin/Fz4 signaling (24). The tip cell markers Apln and Esm1 (21, 25) were overrepresented in the *Z/Edn2;Six3-Cre* retina transcriptome along with Vegfa, which was expected for an hypoxic retina (Fig. 4 *B* and *C*). The abundances of several other transcripts, including potassium channel Kcne3 transcripts, were also substantially increased. The failure to observe statistically significant enrichment of other tip cell transcripts in our *Z/Edn2;Six3-Cre* transcriptome analyses may reflect the use of whole retina rather than purified ECs as the starting material.

The spatial distributions of several of these differentially regulated transcripts were analyzed by in situ hybridization to cross-sections and flat mounts of P6 eyes (Fig. 4 *D*–*O*). In control eyes, Apln transcripts are localized to a thin annulus of tip cells at the growing vascular front, whereas in *Z/Edn2;Six3-Cre* retinas, they are distributed over the outer one-half of the thickened donut-shaped vascular plexus as well as in a dispersed set of cells beyond the vascular front, possibly a subset of astrocytes (Fig. 4 *D* and *L*). In cross-sections of the midcentral retina, Dll4 and Ang2 transcripts, both of which are normally enriched in tip cells (21), are present at the vitreal face of *Z/Edn2;Six3-Cre* but undetectable in the corresponding region of control retinas (Fig. 4 *E* and *F*). In flat mounts of control retinas, Dll4 transcripts are localized to tip cells, whereas in *Z/Edn2;Six3-Cre* retinas, Dll4 transcripts are seen throughout the thickened vascular plexus (Fig. 4*K*). Apj transcripts, which are localized to veins and mature capillaries in control retinas, are confined to a sparsely vascularized central territory in *Z/Edn2;Six3-Cre* retinas and excluded from the surrounding mass of ECs (Fig. 4*M*). Plexin-D1 transcripts, which are enriched at the vascular front in control retinas (26), and Kcne3 transcripts, which localize to tip cells in control retinas, are both found throughout the thickened vascular plexus in *Z/Edn2;Six3-Cre* retinas (Fig. 4 *N* and *O*).

During normal ocular development, astrocytes ahead of the radially expanding vascular plexus express *Vegfa* (2). After the vitreal face of the retina has been vascularized, cells within the INL, particularly Muller glia, serve as the principle source of Vegfa. At P6, Vegfa transcripts in *Z/Edn2;Six3-Cre* retinas are up-regulated in both the INL and astrocytes (Fig. 4*G*, *Right*). The endothelial localization of Apln transcripts and the periendothelial localization of Vegfa transcripts are shown in retina cross-sections (Fig. 4 *H* and *I*). At P6, control retinas show Vegf transcripts both in front of the growing vasculature and within circumscribed territories bounded by arteries and arterioles in the more mature central retina (Fig. 4 *J*). In contrast, *Z/Edn2;Six3-Cre* retina flat mounts show Vegf transcripts at uniformly high abundance throughout the central retina (Fig. 4 *J*). In *Z/Edn2;Six3-Cre* retinas, the high levels of Vegfa expression by astrocytes that are in intimate contact with nonperfused ECs argue that, during normal retinal vascular development, repression of astrocyte-derived Vegfa is not caused by direct EC–astrocyte contact but rather by the increased astrocyte oxygenation that accompanies the radial expansion of a perfused vasculature. The data also show that the block to vascular growth in *Z/Edn2;Six3-Cre* retinas is

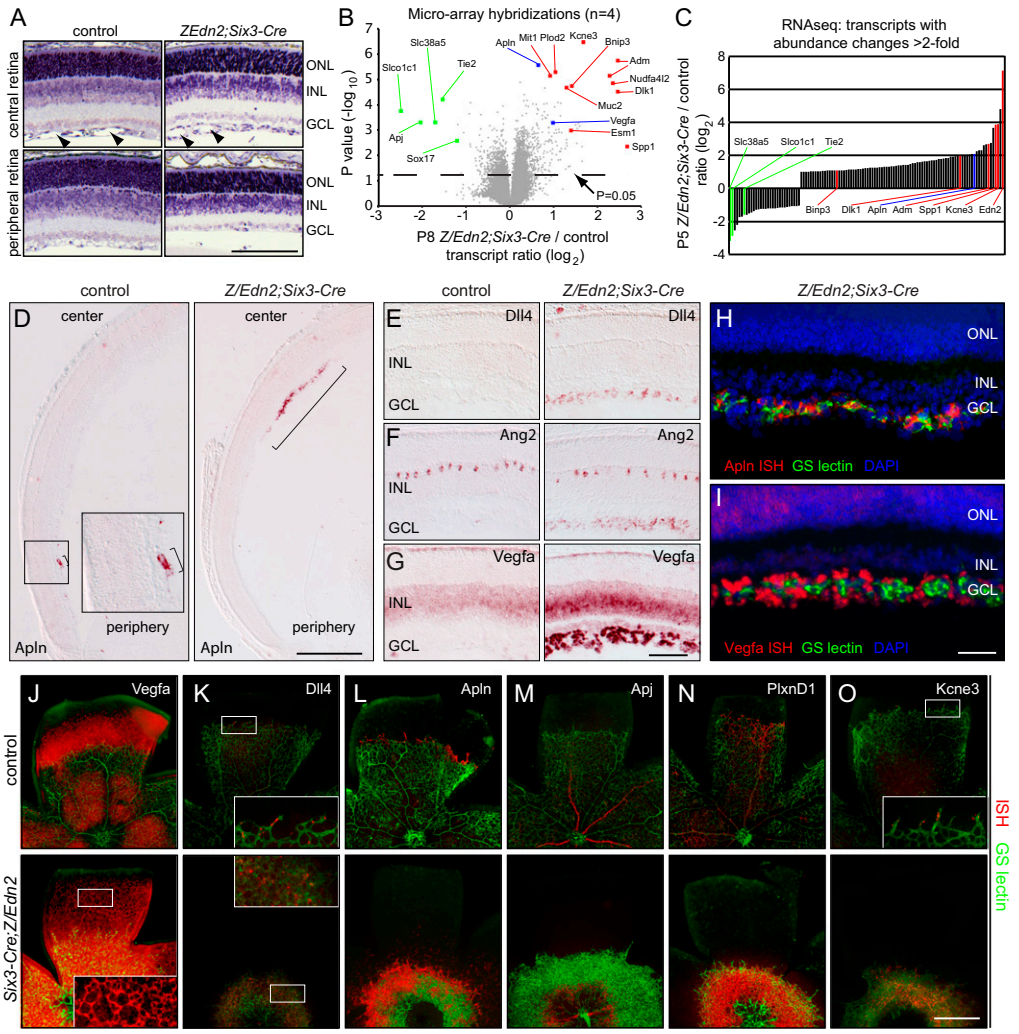

Fig. 4. Altered expression of genes involved in vascular development in *Z/Edn2;Six3-Cre* retinas. (*A*) Sections of central and peripheral P6 control and *Z/Edn2;Six3-Cre* retinas stained with Toluidine Blue. In the *Z/Edn2;Six3-Cre* retina, patent blood vessels are observed on the vitreal face of the central retina (arrowheads), but the peripheral retina is avascular. Except for thinning in the periphery, the morphology of the *Z/Edn2;Six3-Cre* retina is largely normal. (Scale bar: 100 μm.) (*B*) Microarray hybridization with total retina RNA from four biologically independent pairs of P8 control and *Z/Edn2;Six3-Cre* samples. In the volcano plot, probe sets showing more than twofold reduction in hybridization intensity in the *Z/Edn2;Six3-Cre* sample and a *P* value < 0.05 are shown in green, and probe sets showing more than twofold increase in hybridization intensity in the *Z/Edn2;Six3-Cre* sample and a *P* value < 0.05 are shown in red. Blue symbols represent *Apln* and *Vegfa* probe sets, which show an approximately twofold increase in hybridization intensity and *P* values < 0.05. In situ hybridization for these two transcripts is shown in *D* and *G*. Because of the presence of nonspecific background signal, microarray hybridization intensity changes typically underestimate the actual fold change in RNA abundance. (*C*) Expression profiling using RNAseq. The data presented is from a single sequencing experiment with RNA from P5 control and *Z/Edn2;Six3-Cre* retinas. The ratio (on a $\log_2$ scale) of read counts for individual transcripts from control vs. *Z/Edn2;Six3-Cre* libraries is shown for all genes with more than twofold ratios (i.e., $\log_2 > 1$) and *P* values < 0.05. Transcripts highlighted in *B* are highlighted here. (*D–I*) In situ hybridization to retina sections from P6 control and *Z/Edn2;Six3-Cre* retinas. Probes for tip cell markers are (*D*) Apln, (*E*) Dll4, and (*F*) Ang2. In *D*, Apln transcripts are present only on the vitreal face of the retina. They are localized to a narrow annulus of tip cells in the periphery of the control retina (bracket in boxed region enlarged in *Inset* in *D*, *Left*) but broadly distributed in surface ECs near the center of the *Z/Edn2;Six3-Cre* retina (*D*, *Right*). *E–I* show sections of central retina. In *E*, Dll4 transcripts are not detectable in the control retina but localize to ECs on the vitreal surface of the *Z/Edn2;Six3-Cre* retina. In *F*, Ang2 transcripts are present in a subset of cells in the INL (probably horizontal cells) in both control and *Z/Edn2;Six3-Cre* retinas; Ang2 transcripts are absent from ECs in the control retina and present in ECs on the vitreal surface of the *Z/Edn2;Six3-Cre* retina. In *G*, Vegfa transcripts are present in the retinal pigment epithelium (RPE) and INL in both control and *Z/Edn2;Six3-Cre* retinas (with a stronger INL signal in the latter); Vegfa transcripts are not detected on the vitreal surface of the control retina but are abundant in astrocytes in *Z/Edn2;Six3-Cre* retinas. In *H* and *I*, GS-lectin staining after in situ hybridization to *Z/Edn2;Six3-Cre* retinas shows (*H*) Apln transcripts colocalizing with GS-lectin in ECs and (*I*) Vegfa transcripts in astrocytes interdigitating with ECs. ISH, in situ hybridization. (Scale bars: *D*, 500 μm; *E–G*, 100 μm; *H* and *I*, 50 μm.) (*J–O*) In situ hybridization to retina flat mounts from P6 control and *Z/Edn2;Six3-Cre* retinas. Green, GS-lectin; red, in situ hybridization signal. Boxed regions are enlarged as *Insets*. The in situ hybridization signal in *H–O* and Fig. 6*A* consists of purple alkaline phosphatase reaction product; it has been false colored red for illustrative purposes. (Scale bar: 500 μm.) PlxnD1, Plexin-D1.

not caused by a lack of Vegfa but, on the contrary, occurs despite elevated Vegfa.

To summarize the experiments up to this point, early pan-retinal expression of Edn2 produces a large excess of tip cells within the growing vasculature; however, these cells do not spread radially beyond the central retina, and they do not invade the retina, despite high levels of local (astrocyte) and intraretinal (INL) *Vegfa* expression.

Low Levels of Edn2 Generate Interstitial Tip Cells in the Mature Retinal Vasculature. Because the *Six3-cre* driver recombines target genes in all retinal neurons and glia, including astrocytes (as determined by crossing it to a reporter line) (Fig. S3*A*) (27), we wondered whether less complete recombination of the *Z/Edn2* target might lead to a milder vascular phenotype and permit an assessment of Edn2 effects in the context of a minimally perturbed retinal vascular architecture. To achieve this goal, we studied *Z/Edn2;PDGFRα-Cre* mice, in which recombination of the *Z/Edn2* target peaks at ∼30% of retinal cells, which was measured using *Z/H2B-GFP*, a reporter identical in all respects to *Z/Edn2* except for the replacement of *Edn2* by histone *H2B-GFP* coding sequences (Fig. S4*A*). The *Z/Edn2;PDGFRα-Cre* retina closely resembles the WT control with respect to thickness, lamination, and vascular architecture (Fig. S4*B*). However, close inspection of GS-lectin–stained adult retina cross-sections shows that intraretinal capillaries are larger and more numerous in *Z/Edn2;PDGFRα-Cre* retinas compared with controls, an im-

pression confirmed by quantification of OPL capillary density, which showed an ~15% difference in density (Fig. 5*C*). In situ hybridization shows a small elevation in the levels of Vegfa transcripts in the *Z/Edn2;PDGFRα-Cre* INL, especially in regions >10–15 μm from a capillary (Fig. S4*B*).

The data described in the preceding paragraph imply that *Z/Edn2;PDGFRα-Cre* retinas have a modest defect in INL perfusion, despite an elevated capillary density. The resolution to this apparent paradox is that *Z/Edn2;PDGFRα-Cre* retinas have large numbers of capillaries that terminate with blind endings, an architecture that was not observed in either phenotypically normal control retinas or retinas with underdeveloped OPL and IPL capillary beds (Fig. 5 *A* and *B*). [The latter retinas were generated by artificially delaying the expression of the Fz4 ligand Norrin in a genetic background in which the gene coding for Norrin (*Ndp*) was mutated (*Ndp^{KO};Z/Norrin;Glast-CreER*) (figure 7 in ref. 28).] The blind endings were most numerous in the IPL, with ~200 per retina. Blind endings were typically decorated with multiple filopodia, and immunostaining for the stalk cell marker Tie2 showed that, unlike the bulk of the intraretinal capillary network, the blind endings were selectively depleted for Tie2 (Fig. 5*A*). A comparison of the number of blind endings at P12, P13, P20, and P28 in control retinas (n = 30) with *Z/Edn2;PDGFRα-Cre* retinas (n = 20) shows (*i*) that blind endings are present in immature retinas of both genotypes and are most abundant in the IPL and (*ii*) that blind endings are largely eliminated from control but not from *Z/Edn2;PDGFRα-Cre* retinas by P28.

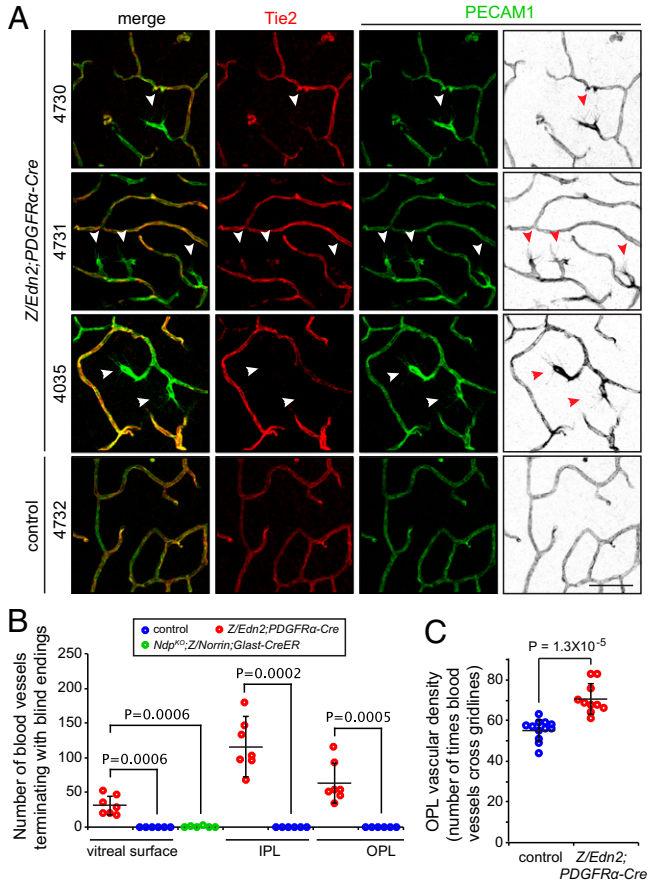

Fig. 5. Interstitial tip cells in adult *Z/Edn2;PDGFRα-Cre* retinas. (*A*) Flat-mount adult control and *Z/Edn2;PDGFRα-Cre* retinas immunostained for Tie2 and PECAM1 were imaged at the level of the OPL. The three *Z/Edn2;PDGFRα-Cre* examples (mouse numbers 4035, 4730, and 4731) show capillaries terminating with blind endings decorated by multiple filopodia (arrowheads) and reduced levels of Tie2. The control mouse (4732) shows only the normal intraretinal capillary plexus. Column 4 shows the anti-PECAM1 images in grayscale, with intensities inverted for greater clarity. Many capillaries that enter or exit the focal plane appear truncated in these images, but these capillaries are readily distinguished from blind endings by examining adjacent focal planes. Additionally, normal adult capillary ECs express Tie2 and lack filopodia. (Scale bar: 50 μm.) (*B*) Quantification of blind endings in adult control and *Z/Edn2;PDGFRα-Cre* retinas. Each symbol represents one retina. Means and SDs are shown. The *Ndp^{KO};Z/Norrin;Glast-CreER* retinas have a several fold lower OPL capillary density than WT control or *Z/Edn2;PDGFRα-Cre* retinas (figure 7 in ref. 28). (*C*) The OPL capillary density in *Z/Edn2;PDGFRα-Cre* retinas is elevated by ~15% compared with control retinas. Relative vascular density was determined by counting the number of intersections of GS-lectin–stained vessels with a set of six parallel lines, each of 500-μm length, within an area of 500 μm^2. Means, SDs, and *P* values are indicated.

These data indicate that the mature *Z/Edn2;PDGFRα-Cre* retinal vasculature harbors large numbers of tip cells embedded within an otherwise normal vascular architecture. We presume that hypoperfusion of the blind endings contributes to tissue hypoxia, which in turn, leads, through Vegfa signaling, to the observed increase in vascular density. However, the presence of filopodia bearing ECs cannot be ascribed simply to tissue hypoxia and/or elevated levels of Vegfa, because *Ndp^{KO};Z/Norrin;Glast-CreER* retinas exhibit similar or greater levels of hypoxia but do not develop interstitial tip cells (28).

Spatial Localization of Edn2 Action. The experiments described thus far involve relatively uniform *Z/Edn2* activation across the retina. We thought it would be of interest to determine the effect on retinal vascular development of a spatially defined pattern of *Z/Edn2* activation. Because vascular growth begins at the optic disk, the simplest experimental design would be one in which *Z/Edn2* is activated exclusively in the peripheral retina, and therefore, the growing vasculature could be studied as it passes from a territory with little or no Edn2 to one with excess Edn2. To effect this experimental design, we used a *Pax6-α-Cre* driver, because this transgene recombines target genes in all retinal layers beginning at ~E11 but only in the nasal and temporal ~50% of the retina (29). Using a reporter, recombination is observed in all retinal neurons and Muller glia but not in astrocytes (Fig. S3*B*). The *Z/Edn2;Pax6-α-Cre* retinal architecture is close to normal in the central retina, with three vascular layers and only irregular pockets of *Vegfa* expression in the INL (Fig. 6*A*, *Left*). However, in the peripheral *Z/Edn2;Pax6-α-Cre* retina, intraretinal capillaries were rarely observed, there was massive induction of Vegfa in the INL, and as observed in *Z/Edn2;Six3-Cre* retinas, there was thinning of all three retinal layers (Fig. 6*A*, *Right*).

Direct measurements of tissue hypoxia by immunostaining for Hypoxyprobe in retinal cross-sections showed little accumulation in the INL of the central *Z/Edn2;Pax6-α-Cre* retina but substantial accumulation in the INL of the peripheral retina, especially in those territories farthest removed from a blood vessel (Fig. 6*A*, *Lower*). Flat-mount imaging confirmed this trend, showing a pattern of Hypoxyprobe accumulation in irregularly shaped territories that were bounded by narrow perivascular bands of Hypoxyprobe-negative retina (Fig. 6*B*).

The block to vascular growth in the periphery of the *Z/Edn2;Pax6-α-Cre* retina creates a sharp boundary between the fully vascularized central retina and the completely avascular peripheral retina. Just proximal to the arrested front, the adult retinal vasculature looks essentially normal, but at the front, there are numerous filopodia-bearing and Tie2-negative ECs (i.e., a layer of tip cells ahead of a plexus of stalk cells) (Fig. 6*C*). The simplest explanations for this arrangement are that Edn2-expressing retinal tissue favors the tip cell state while blocking tip cell migration and that this spatial arrangement of tip and stalk cell states can persist into adulthood. Because tip cells are only seen at the vascular front in *Z/Edn2;Pax6-α-Cre* retinas, it seems

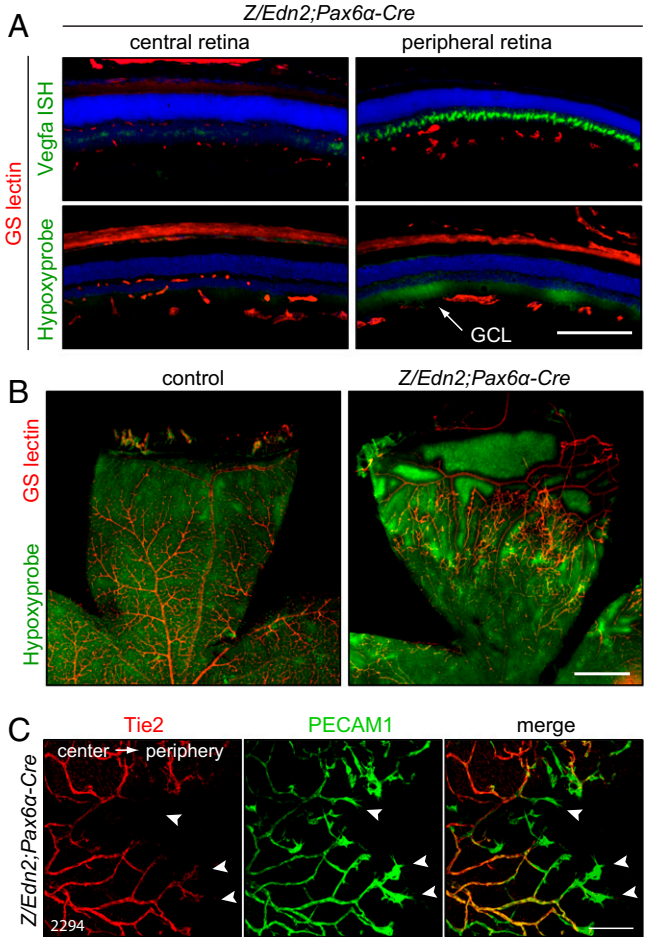

Fig. 6. Spatially localized Edn2 expression results in local inhibition of retinal vascular development. (*A*, *Upper*) Sections of *Z/Edn2;Pax6α-Cre* retinas stained with GS-lectin after Vegfa in situ hybridization. (*A*, *Lower*) *Z/Edn2;Pax6α-Cre* retinas immunostained for Hypoxyprobe. (*A*, *Left*) Vascular architecture appears close to normal in the central retina, where *Pax6α-Cre* is not expressed; there is a low level of Vegfa expression in the INL and a low level of Hypoxyprobe accumulation. (*A*, *Right*) Hypertrophic blood vessels on the vitreal face of the retina with attenuated intraretinal projections are seen in the peripheral retina, where Cre-mediated recombination has activated Edn2 expression from the *Z/Edn2* locus. This region has high expression of Vegfa in Muller glia and high levels of Hypoxyprobe. (Scale bar: 200 μm.) (*B*) Flat mount of control and *Z/Edn2;Pax6α-Cre* retinas stained for Hypoxyprobe and GS-lectin. (Scale bar: 500 μm.) (*C*) The front of the IPL vasculature in an adult *Z/Edn2;Pax6α-Cre* retina immunostained for Tie2 and PECAM1. Arrowheads point to several ECs at the vascular front that are decorated with filopodia and express low levels of Tie2. The retinal center is to the left, and the periphery is to the right. (Scale bar: 100 μm.)

that locally synthesized Edn2 and its effectors (discussed below) exhibit little diffusion across the retina.

Vascular Effects of Edn2 Are Mediated by Retinal Neurons and/or Glia via Ednra Signaling. The experiments described thus far have not defined the cell types that serve as the proximal sites of Edn2 action. The simplest model would be one in which retina-derived Edn2 acts directly on the growing vasculature, but it is also possible that Edn2 acts on nonvascular cells, which then signal secondarily to ECs. To distinguish between these possibilities, we used the *Pax6-α-Cre* driver to both activate *Z/Edn2* and eliminate either of the two endothelin receptors in the peripheral retina. For this purpose, we constructed a mouse line carrying a conditional null allele of Ednrb ($Ednrb^{f}$) (Fig. S1*B*), and we used a previously described $Ednra^{f}$ line (30). Because *Pax6-α-Cre* is active in the neural retina but not in the vasculature or astrocytes (Fig. S3*B*), this experiment asks two questions. Does Edn2 mediate its vascular affects by acting on retinal neurons and/or glia? If so, do those effects involve signaling through only one of two endothelin receptors? To increase the efficiency of Cre-mediated elimination of receptor gene function, these experiments were conducted with genotypes that required only a single Cre-mediated deletion event to eliminate receptor function (i.e., $Ednra^{f/-}$ or $Ednrb^{f/-}$ rather than $Ednra^{f/f}$ or $Ednrb^{f/f}$). Littermates carrying $Ednra^{f/+}$ or $Ednrb^{f/+}$ served as controls.

Fig. 7*A* shows the result of *Ednra* or *Ednrb* elimination. The adult retina flat mounts show the trilayered vasculature (color coded by depth) as well as the boundary between Cre-recombined and -nonrecombined retinal territories. This boundary can be precisely defined, because the *Z/Edn2* allele includes the coding region for a β-gal reporter within the *loxP-stop-loxP* cassette, and therefore, β-gal is produced by cells lacking Cre and is eliminated from cells expressing Cre. As seen in the control *Z/Edn2;Pax6-α-Cre;*$Ednrb^{f/+}$ retina, the two intraretinal vascular beds occupy a territory that closely matches the territory of β-gal expression (Fig. 7*A*, *Left*). The hypertrophic surface vasculature continues for a variable distance beyond this border. By contrast, elimination of *Ednra* in the retina (genotype *Z/Edn2;Pax6-α-Cre;* $Ednra^{f/-}$) leads to growth of all three vascular layers beyond the Cre-recombined territory, whereas loss of *Ednrb* in the retina (genotype *Z/Edn2;Pax6-α-Cre;*$Ednrb^{f/-}$) leads to truncation of the two intraretinal vascular layers several hundred micrometers short of the edge of the Cre-recombined territory, with variable growth of the surface vasculature beyond that point (Fig. 7*A*, *Center* and *Right*).

These phenotypes were quantified by measuring total retinal area and the fraction of the retinal plane that is vascularized for *Z/Edn2;Pax6-α-Cre;*$Ednra^{f/-}$, *Z/Edn2;Pax6-α-Cre;*$Ednra^{f/+}$, *Z/Edn2;Pax6-α-Cre;*$Ednrb^{f/-}$, and *Z/Edn2;Pax6-α-Cre;*$Ednrb^{f/+}$ retinas (Fig. 7 *B* and *C*). This analysis shows that elimination of *Ednra* in retinal neurons and glia results in a nearly complete rescue of the vascular truncation phenotype. In contrast, elimination of *Ednrb* in retinal neurons and glia seems to sensitize the vasculature to Edn2-mediated inhibition, as determined by the arrest of vascular growth proximal to the front of Cre-mediated recombination (Fig. 7*A*) and the smaller total area of vascularized retina (Fig. 7 *B* and *C*). This last observation could be explained if Ednra and Ednrb act antagonistically or if loss of Ednrb leads to a compensatory upregulation of Ednra or a sensitization of its signaling pathway.

Tissue and Developmental Stage Specificity of the Antiangiogenic Effects of Edn2. The phenotypic analyses described thus far were confined to the retina, and thus, they do not address whether Edn2-dependent inhibition of vascular growth is observed in other tissues. To the best of our knowledge, the expression of the *Pax6-α-Cre* is confined to the retina, but *Six3-Cre* is also expressed in the embryonic forebrain (31), and *PDGFRα-Cre* expression would be expected in a wide variety of tissues (32). The postnatal viability and grossly normal health of *Z/Edn2;Six3-Cre* and *Z/Edn2;PDGFRα-Cre* mice argue against a severe Edn2-mediated inhibition of extraretinal vascular development in these two lines. To test the effect of Edn2 overexpression at the beginning of vascular development, *Z/Edn2* was combined with *Sox2-Cre*, a transgene that expresses Cre throughout the early embryo. As shown in Fig. 8 *A–F* and Table 1, *Z/Edn2;Sox2-Cre* embryos recovered at E8.5 were mildly growth-retarded, but *Z/Edn2;Sox2-Cre* embryos recovered at E9.5–E10.5 were severely retarded and displayed an open neural tube, an enlarged heart, and pooled blood in the head and thorax. Strikingly, flat-mount immunostaining for PECAM1 showed a nearly complete absence of vascular development in E9.5 *Z/Edn2;Sox2-Cre* embryos (Fig. 8 *G* and *H*). *Z/Edn2*-dependent growth retardation during fetal life could be suppressed in ∼20% of late-gestation embryos

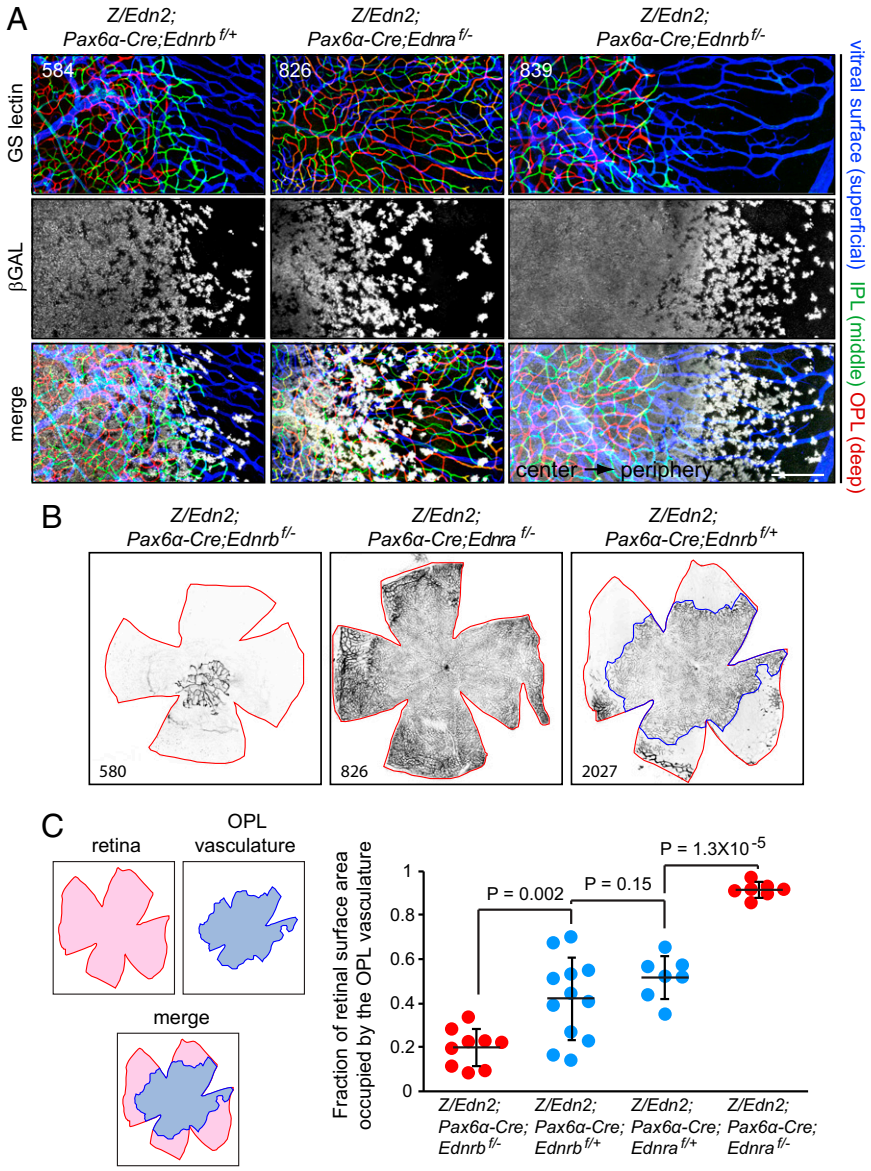

Fig. 7. Inhibition of vascular development in *Z/Edn2;Pax6α-Cre* retinas requires expression of *Ednra* in the neural retina. (*A*) Flat-mount retinas immunostained for β-gal (white; expressed from the *Z/Edn2* locus in the absence of Cre-mediated recombination) and costained with GS-lectin. In this Z-stacked image, the three vascular layers are color-coded blue, green, and red for depth. The retinal center is to the left, and the periphery is to the right. A sharp border between the zones of Cre expression and nonexpression in the neural retina is evident from the distribution of β-gal. (Scale bar: 200 μm.) (*B*) Flat mounts showing the extent of OPL vascular coverage in retinas with various Ednr conditional and null alleles on a background of *Z/Edn2;Pax6α-Cre*. Because Cre-mediated recombination of the *Ednra* and *Ednrb* conditional alleles is controlled by *Pax6α-Cre*, their spatiotemporal pattern of recombination should coincide with the recombination pattern of *Z/Edn2* (i.e., recombination in the medial and temporal peripheral neural retina at ∼E11). For the three examples shown, Cre-mediated recombination activates *Z/Edn2* and produces (*Left*) homozygous loss of *Ednrb* (Edn2-dependent inhibition of vascular development is enhanced), (*Right*) heterozygous loss of *Ednrb* (the extent of Edn2-dependent inhibition of vascular development is very similar to the extent of inhibition seen with the full complement of Ednr alleles), or (*Center*) homozygous loss of *Ednra* (Edn2-dependent inhibition of vascular development is fully suppressed). Red, outline of the retina. (*C*) Quantitative analysis of OPL vascular coverage in retinas with various Ednr-conditional alleles and null alleles on a background of *Z/Edn2;Pax6α-Cre*. Diagrams in *Left* show the outlines of the retinal area (red) and the vascularized OPL territory (blue) for the retina shown in *B*, *Right*. Each symbol in the plot represents one retina. Means and SDs are shown.

by eliminating *Ednra* but not *Ednrb* (Fig. 8*J* and Table 1). In fact, the ∼20% figure is a substantial underestimate of the *Ednra* effect, because among the *Sox2-Cre;Ednra*$^{f/-}$ littermates of the *Z/Edn2;Sox2-Cre;Ednra*$^{f/-}$ embryos, the loss of *Ednra* alone resulted in only ∼20% survival to late gestation. The phenotypic rescue conferred by mutation of *Ednra* shows that, in the embryo (like in the retina), overexpression of Edn2 does not produce nonspecific toxicity but rather, exerts its effect by engaging one of its two high-affinity receptors.

To extend the testing of Edn2 overexpression to later times and additional tissues, we examined the vasculature in *Z/Edn2;K5-Cre* and *Z/Edn2;Foxg1-Cre* mice, in which Cre production begins at or shortly after midgestation in the epidermis (33) and before midgestation in the head, respectively (34). Sections of postnatal skin from *Z/Edn2;K5-Cre* mice and late-gestation brains from *Z/Edn2;Foxg1-Cre* fetuses show vascular architecture indistinguishable from normal littermate controls (Figs. S5 and S6). In X-Gal–stained sections through the external ear, control *Z/Edn2* mice produce β-gal in the epidermis from the unrecombined *Z/Edn2* locus, control *K5-Cre* mice show no β-gal in the epidermis, and *Z/Edn2;K5-Cre* mice show both a loss of epidermal β-gal and a massive increase in dermal pigmentation (Fig. S5). The increase in pigmentation is the expected result of Ednrb hyperactivation in melanocyte precursors (35, 36), and it serves as an internal control for the production of bioactive Edn2. An analogous internal control is observed in *Z/Edn2;Foxg1-Cre* mice, where excess Edn2 production in the head results in a failure to close the palate and eyelids; the former defect produces early postnatal lethality (Fig. S6).

Taken together, these data show that the antiangiogenic effects of Edn2 are far from universal, despite the expression of Ednra and Ednrb in a wide range of cell types, including neurons, keratinocytes, adipocytes, and smooth muscle cells (17). Indeed, even closely related tissues, such as brain and retina, differ markedly in their response to Edn2.

Edn Signaling in the Normal Retina: Genetic Loss-of-Function Experiments. All of the experiments described thus far involve overexpression of Edn2. If endothelin signaling plays a nonredundant role in normal retinal vascular development or homeostasis, one would expect that loss of endothelin signaling would produce defects in vascular architecture. To test this prediction, we generated a conditional null allele of *Edn2* (Fig. S1*C*). *Edn2*$^{-/-}$ mice (derived by germ-line recombination of the

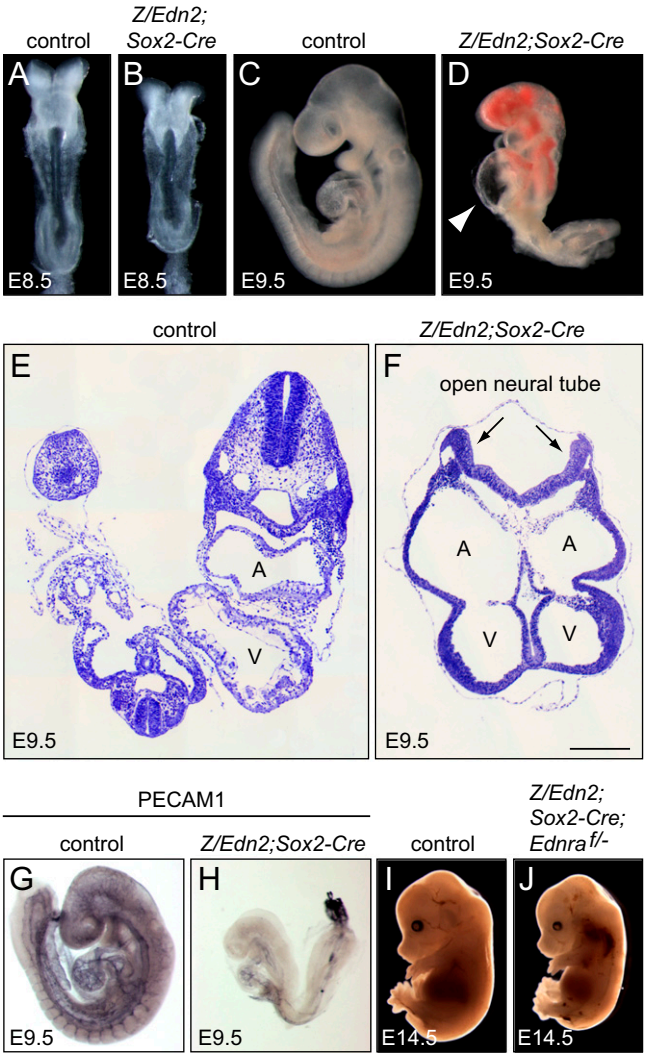

Fig. 8. Inhibition of vascular development and midgestational lethality in *Z/Edn2;Sox2-Cre* embryos. (*A* and *B*) Dorsal view of E8.5 control and *Z/Edn2; Sox2-Cre* embryos, showing mild growth retardation in the *Z/Edn2;Sox2-Cre* embryo. (*C* and *D*) Lateral view of E9.5 control and *Z/Edn2;Sox2-Cre* embryos, showing severe growth retardation in the *Z/Edn2;Sox2-Cre* embryo, with pooling of blood in the head and thorax and dilated cardiac chambers (arrowhead in *D*). (*E* and *F*) Transverse sections of Toluidine Blue-stained E9.5 control and *Z/Edn2;Sox2-Cre* embryos. (*E*) The control embryo has distinct atrial and ventricular chambers and a closed neural tube. (*F*) The *Z/Edn2; Sox2-Cre* embryo has greatly enlarged and partially distinct atrial and ventricular chambers and an open neural tube. (Scale bar: 200 μm.) (*G* and *H*) Flat-mount PECAM1 staining (with an HRP-conjugated secondary antibody and purple/black reaction product) of E9.5 control and *Z/Edn2;Sox2-Cre* embryos. (*G*) The control embryo shows a well-organized segmental vasculature. (*H*) The *Z/Edn2;Sox2-Cre* embryo shows minimal vascular development. (*I* and *J*) Deletion of *Ednra* can rescue the midgestational growth retardation of *Z/Edn2;Sox2-Cre* embryos, which is shown by the normal appearance of the E14.5 *Z/Edn2;Sox2-Cre;Ednra*$^{fl/-}$ embryo.

conditional *Edn2* allele) are runted and die at 3–4 wk of age, but their retinal vascular architecture appears normal. Retinal vascular architecture was also unaffected in *Edn2*$^{fl/-}$*;Six3-Cre* mice. Because Edn1 (which activates Ednra and Ednrb) and/or Edn3 (which activates Ednrb) could be compensating for loss of Edn2, we also studied vascular architecture in neural retina-specific Ednr KOs: *Ednra*$^{fl/-}$*;Six3-Cre*, *Ednrb*$^{fl/-}$*;Six3-Cre*, and *Ednra*$^{fl/f}$*; Ednrb*$^{f/f}$*;Six3-Cre*. All have normal vascular architecture. Assuming that the Cre recombinase eliminated all four conditional alleles in the double receptor conditional KO, this experiment shows that endothelin signaling by retinal neurons and glia is dispensable for normal vascular development. Taken together, these experiments imply that, in mice, any role that endothelin signaling plays in normal retinal vascular development is redundant with other signaling systems.

Discussion

The principle results of this study are that (*i*) overexpression of Edn2 in the mouse retina leads to an excess of tip cells and inhibition of vascular growth, effects that require Ednra but not Ednrb signaling in retinal neurons and/or glia; (*ii*) overexpression of Edn2 has no effect on vascular architecture in the brain or skin, but it arrests vascular development in the midgestation embryo; and (*iii*) loss of Ednra and/or Ednrb in the retina has little or no effect on normal vascular development. Although the tip cell overproduction/stabilization phenotype described here is reminiscent of the phenotype seen after EC-specific deletion of *Vegfr-3* or suppression of Notch signaling (6, 37, 38), it is conceptually distinct in that it is induced by genetic manipulations of retinal neurons and glia rather than ECs.

Implications for Tip Vs. Stalk Cell States. As noted above, Notch and Vegfr-3 signaling in ECs controls the balance between tip and stalk cell states. Notch signaling is largely intrinsic to the vasculature, reflecting tip vs. stalk cell production of ligands Dll4 and Jagged1 and their relative occupancies of Notch receptors on the same cells (6, 39). Vegfa signaling integrates EC growth with tissue hypoxia: a gradient of Vegfa guides tip cell migration, and the absolute levels of Vegfa determine stalk cell proliferation (3). Cross-regulation between the two signaling systems occurs through Vegf-dependent regulation of Notch signaling and Notch regulation of Vegfr-3 levels (37, 38). Notch/Vegf cross-regulation also involves other signaling systems; Vegfa induces plexin-D1 expression by tip cells, and the resulting Sema-3E/Plexin-D1 signal represses Notch signaling (26).

Table 1. Embryonic phenotypes of *Z/Edn2;Sox2-Cre* and *Z/Edn2; Sox2-Cre* combined with mutation of *Ednra* or *Ednrb*

Genotype	Observed	Expected
E9.5–E10.5 embryos showing normal development from the cross *Sox2-Cre/Sox2-Cre* (male) × *Z/Edn2/+* (female)		
Z/Edn2;Sox2-Cre	0	44
Sox2-Cre	44	44
E9.5–E10.5 embryos showing normal development from the cross *Ednrb*$^{+/-}$*;Sox2-Cre/Sox2-Cre* (male) × *Z/Edn2/+;Ednrb*$^{f/f}$ (female)		
Z/Edn2;Sox2-Cre;Ednrb$^{f/-}$	0	16
Z/Edn2;Sox2-Cre;Ednrb$^{f/+}$	0	16
Sox2-Cre;Ednrb$^{f/-}$	9	16
Sox2-Cre;Ednrb$^{f/+}$	16	16
E11.5–E18.5 embryos showing normal development from the cross *Ednra*$^{+/-}$*;Sox2-Cre/Sox2-Cre* (male) × *Z/Edn2/+;Ednra*$^{f/f}$ (female)		
Z/Edn2;Sox2-Cre;Ednra$^{f/-}$	5	26
Z/Edn2;Sox2-Cre;Ednra$^{f/+}$	0	26
Sox2-Cre;Ednra$^{f/-}$	5	26
Sox2-Cre;Ednra$^{f/+}$	26	26

For each cross, the expected number of embryos is determined by the genotypic class that has no perturbation or the most minimal perturbation in endothelin signaling components.

Can the effects of Edn2 overexpression be understood within the existing framework of EC development? The simplest hypothesis is that Edn2 acting on retinal neurons and/or glia causes the production of one or more factors that arrest vascular migration and invasion. The resulting tissue hypoxia leads to up-regulation of astrocyte- and retina-derived Vegfa, which promotes both the tip cell state and stalk cell proliferation. Although this model accounts for some of the data, it does not explain the persistence of occasional tip cells within the mature retinal vasculature of *Z/Edn2;PDGFRα-Cre* mice. This model also does not account for the observation that other mutant retinas with impaired vascular growth and elevated levels of Vegfa (e.g., Ndp^{KO} and Ndp^{KO}*;Z/Norrin;Glast-CreER*) do not exhibit an excess of tip cells (Fig. 5) (28).

Properties of the Tissue Mediator(s) of Endothelin Effects on Vascular Development. The production of excess tip cells in the context of increased endothelin signaling suggests that retinal neurons and/or glia produce a tip cell factor (or factors) and that this factor is distinct from Vegfa. Whether a single factor or multiple factors account for both the excess of tip cells and the block to EC migration and invasion is unknown. It is also unclear whether such activities derive from cell-associated or -secreted factor(s). If the factor is secreted, the sharp boundary of EC invasion and growth inhibition seen in *Z/Edn2;Pax6-α-Cre* retinas argues that its diffusion is limited. The failure to observe a vascular phenotype when the developing brain and epidermis are exposed to Edn2 (in *Z/Edn2;Foxg1-Cre* and *Z/Edn2;K5-Cre* mice, respectively) implies that the brain and epidermis differ from the retina in their response to endothelin or their intrinsic capacity to produce the migration/invasion blocking factor(s).

One of the most striking features of the Edn2 overexpression phenotype is its ability to override the normal homeostatic mechanisms that control retinal vascular development, including Vegfa-induced migration and invasion. This effect is especially striking, because in these experiments, ECs were not subject to genetic manipulation. Based on the potency of its effects, the data suggest that this undefined mode of communication between the neural retina and the vasculature may be a major regulator of vascular growth and development.

Clinical Implications. In *Z/Edn2;PDGFRα-Cre* mice, the presence of interstitial tip cells in what is otherwise a nearly normal retinal vasculature implies that many or all adult capillary ECs retain the capacity to transition to a tip cell state. Such a capacity may be relevant to the initiation of neovascular growth, which is seen in diabetic retinopathy or retinopathy of prematurity. If, as suggested here, the retina produces one or more tip cell factors and if such factors could be identified, it would be of great interest to explore their roles in diseases associated with pathologic neovascularization.

Methods

Gene targeting, mouse husbandry, RNAseq, microarray hybridization, in situ hybridization, histochemistry, immunostaining, labeling of patent blood vessels, Hypoxyprobe analysis, and quantification of retinal vascular coverage are described in *SI Methods*.

ACKNOWLEDGMENTS. The authors thank Dr. Hugh Cahill for assistance with DiI experiments, Ms. Leila Toulabi for technical assistance, and Dr. Hao Chang and two referees for helpful comments on the manuscript. This work was supported by the National Eye Institute (National Institutes of Health) and the Howard Hughes Medical Institute.

1. Uemura A, Kusuhara S, Katsuta H, Nishikawa S (2006) Angiogenesis in the mouse retina: A model system for experimental manipulation. *Exp Cell Res* 312(5):676–683.
2. Fruttiger M (2007) Development of the retinal vasculature. *Angiogenesis* 10(2):77–88.
3. Gerhardt H, et al. (2003) VEGF guides angiogenic sprouting utilizing endothelial tip cell filopodia. *J Cell Biol* 161(6):1163–1177.
4. Stahl A, et al. (2010) The mouse retina as an angiogenesis model. *Invest Ophthalmol Vis Sci* 51(6):2813–2826.
5. Eilken HM, Adams RH (2010) Dynamics of endothelial cell behavior in sprouting angiogenesis. *Curr Opin Cell Biol* 22(5):617–625.
6. Benedito R, et al. (2009) The notch ligands Dll4 and Jagged1 have opposing effects on angiogenesis. *Cell* 137(6):1124–1135.
7. Potente M, Gerhardt H, Carmeliet P (2011) Basic and therapeutic aspects of angiogenesis. *Cell* 146(6):873–887.
8. Jakobsson L, et al. (2010) Endothelial cells dynamically compete for the tip cell position during angiogenic sprouting. *Nat Cell Biol* 12(10):943–953.
9. Arima S, et al. (2011) Angiogenic morphogenesis driven by dynamic and heterogeneous collective endothelial cell movement. *Development* 138(21):4763–4776.
10. Ye X, Wang Y, Nathans J (2010) The Norrin/Frizzled4 signaling pathway in retinal vascular development and disease. *Trends Mol Med* 16(9):417–425.
11. Gale NW, et al. (2002) Angiopoietin-2 is required for postnatal angiogenesis and lymphatic patterning, and only the latter role is rescued by Angiopoietin-1. *Dev Cell* 3(3):411–423.
12. Ash J, McLeod DS, Lutty GA (2005) Transgenic expression of leukemia inhibitory factor (LIF) blocks normal vascular development but not pathological neovascularization in the eye. *Mol Vis* 11:298–308.
13. Feng Y, et al. (2007) Impaired pericyte recruitment and abnormal retinal angiogenesis as a result of angiopoietin-2 overexpression. *Thromb Haemost* 97(1):99–108.
14. Gariano RF, Gardner TW (2005) Retinal angiogenesis in development and disease. *Nature* 438(7070):960–966.
15. Wang S, Park JK, Duh EJ (2012a) Novel targets against retinal angiogenesis in diabetic retinopathy. *Curr Diab Rep* 12(4):355–363.
16. Yanagisawa M, et al. (1988) A novel potent vasoconstrictor peptide produced by vascular endothelial cells. *Nature* 332(6163):411–415.
17. Kedzierski RM, Yanagisawa M (2001) Endothelin system: The double-edged sword in health and disease. *Annu Rev Pharmacol Toxicol* 41:851–876.
18. Rattner A, Nathans J (2005) The genomic response to retinal disease and injury: Evidence for endothelin signaling from photoreceptors to glia. *J Neurosci* 25(18):4540–4549.
19. Swiderski RE, et al. (2007) Gene expression analysis of photoreceptor cell loss in bbs4-knockout mice reveals an early stress gene response and photoreceptor cell damage. *Invest Ophthalmol Vis Sci* 48(7):3329–3340.
20. Samardzija M, et al. (2012) Activation of survival pathways in the degenerating retina of rd10 mice. *Exp Eye Res* 99:17–26.
21. del Toro R, et al. (2010) Identification and functional analysis of endothelial tip cell-enriched genes. *Blood* 116(19):4025–4033.
22. Li Y, et al. (2008) Direct labeling and visualization of blood vessels with lipophilic carbocyanine dye DiI. *Nat Protoc* 3(11):1703–1708.
23. Raleigh JA, et al. (1987) Fluorescence immunohistochemical detection of hypoxic cells in spheroids and tumours. *Br J Cancer* 56(4):395–400.
24. Ye X, et al. (2009) Norrin, frizzled-4, and Lrp5 signaling in endothelial cells controls a genetic program for retinal vascularization. *Cell* 139(2):285–298.
25. Strasser GA, Kaminker JS, Tessier-Lavigne M (2010) Microarray analysis of retinal endothelial tip cells identifies CXCR4 as a mediator of tip cell morphology and branching. *Blood* 115(24):5102–5110.
26. Kim J, Oh WJ, Gaiano N, Yoshida Y, Gu C (2011) Semaphorin 3E-Plexin-D1 signaling regulates VEGF function in developmental angiogenesis via a feedback mechanism. *Genes Dev* 25(13):1399–1411.
27. Muzumdar MD, Tasic B, Miyamichi K, Li L, Luo L (2007) A global double-fluorescent Cre reporter mouse. *Genesis* 45(9):593–605.
28. Wang Y, et al. (2012b) Norrin/Frizzled4 signaling in retinal vascular development and blood brain barrier plasticity. *Cell* 151(6):1332–1344.
29. Marquardt T, et al. (2001) Pax6 is required for the multipotent state of retinal progenitor cells. *Cell* 105(1):43–55.
30. Ruest LB, Clouthier DE (2009) Elucidating timing and function of endothelin-A receptor signaling during craniofacial development using neural crest cell-specific gene deletion and receptor antagonism. *Dev Biol* 328(1):94–108.
31. Furuta Y, Lagutin O, Hogan BL, Oliver GC (2000) Retina- and ventral forebrain-specific Cre recombinase activity in transgenic mice. *Genesis* 26(2):130–132.
32. Tallquist M, Kazlauskas A (2004) PDGF signaling in cells and mice. *Cytokine Growth Factor Rev* 15(4):205–213.
33. Berton TR, et al. (2003) Tumor formation in mice with conditional inactivation of Brca1 in epithelial tissues. *Oncogene* 22(35):5415–5426.
34. Hébert JM, McConnell SK (2000) Targeting of cre to the Foxg1 (BF-1) locus mediates loxP recombination in the telencephalon and other developing head structures. *Dev Biol* 222(2):296–306.
35. Hou L, Pavan WJ, Shin MK, Arnheiter H (2004) Cell-autonomous and cell non-autonomous signaling through endothelin receptor B during melanocyte development. *Development* 131(14):3239–3247.
36. Aoki H, et al. (2005) Cooperative and indispensable roles of endothelin 3 and KIT signalings in melanocyte development. *Dev Dyn* 233(2):407–417.
37. Benedito R, et al. (2012) Notch-dependent VEGFR3 upregulation allows angiogenesis without VEGF-VEGFR2 signalling. *Nature* 484(7392):110–114.
38. Tammela T, et al. (2011) VEGFR-3 controls tip to stalk conversion at vessel fusion sites by reinforcing Notch signalling. *Nat Cell Biol* 13(10):1202–1213.
39. Hellström M, et al. (2007) Dll4 signalling through Notch1 regulates formation of tip cells during angiogenesis. *Nature* 445(7129):776–780.